SIAM J. NUMER. ANAL.
Vol. 42, No. 2, pp. 714–737

A FINITE ELEMENT TECHNIQUE FOR SOLVING FIRST-ORDER PDEs IN L^P*

J. L. GUERMOND†

Abstract. An approximation technique for solving first-order PDEs in $L^p(\Omega)$, $1 \leq p < +\infty$, is proposed. The method is a generalization of the least-squares method to non-Hilbertian settings. A priori and a posteriori error estimates are proven. Numerical tests in $L^1(\Omega)$ show that this type of technique can handle discontinuities without resorting to limiting procedures.

Key words. finite elements, least-squares, first-order PDEs, nonsmooth optimization

AMS subject classifications. 65N35, 65N22, 65F05, 35J05

DOI. 10.1137/S0036142902417054

1. Introduction.

Given a linear, first-order PDE in a domain $\Omega \subset \mathbb{R}^d$,

$$Lu = f, \tag{1.1}$$

with suitable boundary conditions, the objective of this paper is to present an approximation technique that can handle right-hand sides in $L^1(\Omega)$ and, more generally, right-hand sides in $L^p(\Omega)$, $1 \leq p < +\infty$.

1.1. Introductory comments.

The number of attempts at approximating (1.1) directly in $L^1(\Omega)$ seem to be extremely few (see the series of papers by Lavery [29, 30, 28] and the iteratively reweighted least-squares method of Jiang [23] and [24, Chap. 9]) or seem to have encountered some theoretical difficulties (see [32]). This is in sharp contrast with the fact that an enormous amount of work has been dedicated to the study of first-order PDEs and their various nonlinear generalizations in $L^1(\Omega)$. The main difficulty is that when expressed directly in $L^1(\Omega)$ the discrete problems consist in minimizing nondifferentiable functionals; see, e.g., [23]. The lack of theory and of practical popular algorithms for minimizing this type of functional is responsible for the general preference of authors to seek an approximate solution in the $L^2(\Omega)$ framework where differentiability rules, and the force of habit has made this point of view an undisputed paradigm. The goal of the present work is to show that, as claimed in Jiang [23], when the right-hand side is really so rough as to not be in $L^2(\Omega)$ but in $L^1(\Omega)$ only or when the coefficients of the differential operator are so rough that the solution is only meaningful in $L^1(\Omega)$, then it really pays off to approximate the solution to (1.1) directly in $L^1(\Omega)$. In this case, the discontinuities of the solution are captured as sharply as the grid permits without resorting to adaptive refinement, and numerical tests reveal that the method is not plagued by spurious over- or undershootings. Contrary to standard stabilized $L^2(\Omega)$-based techniques, the direct $L^1(\Omega)$ approximation does not require additional ad hoc tunable coefficients or limiting procedures (see, e.g., Galerkin least-squares techniques [16, 25, 26], discontinuous

*Received by the editors October 31, 2002; accepted for publication (in revised form) October 20, 2003; published electronically June 4, 2004. This work was supported by the Centre National de la Recherche Scientifique (CNRS) and the Texas Institute for Computational and Applied Mathematics (TICAM), where the author completed the work while visiting from 08/2001–07/2003 under a TICAM Visiting Faculty Fellowship.
http://www.siam.org/journals/sinum/42-2/41705.html
†LIMSI (CNRS-UPR 3152), BP 133, 91403, Orsay, France (guermond@limsi.fr).

Galerkin methods [31, 17], bubble stabilization [13, 3, 14], or subgrid stabilization [20, 21, 15]).

The paper is organized as follows. In section 2, we introduce an abstract problem, together with its discrete counterpart, and we give an abstract convergence result. We reformulate this result in the $L^p(\Omega)$ setting in section 3, and we describe an algorithm for computing the approximate solution in this setting. We illustrate numerically the method in section 4, where we solve transport equations and advection-diffusion equations in mixed form in $L^1(\Omega)$. We record conclusions in section 5.

1.2. Notation. Let Ω be an open, bounded, connected Lipschitz domain in $\mathbb{R}^d$. We denote by $|\Omega|$ the measure of Ω. For every Lebesgue measurable function $v : \Omega \longrightarrow \mathbb{R}^m$, $m \geq 1$, we denote by $v \cdot w$ the Euclidean scalar product in $\mathbb{R}^m$. For $1 \leq p < +\infty$, we denote by $\|v\|_{\ell^p}$ the discrete ℓ^p-norm of v, i.e., $\|v\|_{\ell^p} = (\sum_{1\leq i\leq m} v_i^p)^{\frac{1}{p}}$. As usual, we denote by $L^p(\Omega)^m$ the real Banach space of $\mathbb{R}^m$-valued functions whose pth power is Lebesgue integrable, i.e., $\|v\|_{L^p(\Omega)^m} = (\int_\Omega \|v(x)\|_{\ell^p}^p dx)^{\frac{1}{p}}$. $W^{1,p}(\Omega)$ is the space of functions in $L^p(\Omega)$ whose partial derivatives in the distributional sense can be identified with functions in $L^p(\Omega)$. $L^\infty(\Omega)$ is the real Banach space of essentially bounded functions. Hereafter we identify the dual of $L^1(\Omega)$ with $L^\infty(\Omega)$.

Considering two real numbers A, B, we shall use the expression $A \lesssim B$ to say that there exists a generic positive constant c, independent of the discretization parameters, such that (s.t.) $A \leq cB$.

2. An abstract problem.

2.1. The continuous setting. Let E and F be two Banach spaces with norms $\|\cdot\|_E$ and $\|\cdot\|_F$, respectively. Let $L : E \longrightarrow F$ be a bounded linear operator, i.e., $L \in \mathcal{L}(E;F)$. We denote by $L^* : F' \longrightarrow E'$ its adjoint, where E' and F' are the duals of E and F, respectively. We assume also that L is bijective. Let us recall the following important consequence of Banach's closed range theorem and open mapping theorem (see, e.g., [12, p. 29] or [36, p. 205]).

LEMMA 2.1. *An operator $L \in \mathcal{L}(E;F)$ is bijective if and only if there is a constant $\alpha > 0$ s.t.*

$$\forall u \in E, \quad \alpha\|u\|_E \leq \|Lu\|_F, \tag{2.1}$$

$$\forall f' \in F', \quad (L^* f' = 0) \Rightarrow (f' = 0). \tag{2.2}$$

We want to solve the following problem: For $f \in F$,

$$\begin{cases} \text{find } u \in E \text{ s.t.} \\ Lu = f \quad \text{in } F. \end{cases} \tag{2.3}$$

This problem is well-posed, and (2.1) yields the following stability property:

$$\|u\|_E \leq \frac{1}{\alpha}\|f\|_F.$$

Let us now introduce an alternative formulation of problem (2.3). Let us define the functional $J : E \longrightarrow \mathbb{R}$ s.t. $J(v) = \|Lv - f\|_F$, and consider the following problem:

$$\begin{cases} \text{Find } u \in E \text{ s.t.} \\ J(u) \leq J(v) \quad \forall v \in E. \end{cases} \tag{2.4}$$

It is clear that problems (2.4) and (2.3) are equivalent in the sense that they have the same unique solution.

To gain more insight on the nature of problem (2.4), let us consider the case where F is a Hilbert space.

PROPOSITION 2.1. *If F is a Hilbert space (equipped with the scalar product $(v,w)_F = \frac{1}{2}(\|v+w\|_F^2 - \|v\|_F^2 - \|w\|_F^2)$), the solution to* (2.4) *is also the unique solution to the following problem:*

$$\begin{cases} \text{Find } u \in E \text{ s.t.} \\ (Lu, Lv)_F = (f, Lv)_F \quad \forall v \in E. \end{cases} \tag{2.5}$$

Proof. J and J^2 have the same minimum, J^2 is clearly differentiable, and (2.5) is the first-order condition for optimality. Owing to (2.1), the bilinear form $(Lu, Lv)_F$ is continuous and coercive, and $(f, Lv)_F$ is continuous; hence, existence and uniqueness of the solution are easy consequences of the Lax–Milgram theorem. ∎

Actually, (2.5) is the so-called least-squares formulation of (2.3), and it can also be interpreted as the Galerkin formulation of the problem

$$L^*Lu = L^*f.$$

Hence, (2.4) is a simple generalization of the least-squares method to non-Hilbertian settings.

2.2. The discrete setting. We now look for an approximate solution to (2.4). Let $(E_h)_{h>0}$ be a sequence of finite-dimensional spaces s.t. $E_h \subset E$. We assume that the sequence of spaces $(E_h)_{h>0}$ has some interpolation properties; that is, we assume that there is a dense normed subspace $W \subset E$ and a function $\epsilon(h)$, continuous at zero with $\epsilon(0) = 0$, s.t.

$$\forall v \in W, \quad \inf_{v_h \in E_h} \|v - v_h\|_E \lesssim \epsilon(h)\|v\|_W. \tag{2.6}$$

The discrete counterpart to (2.4) is as follows:

$$\begin{cases} \text{Find } u_h \in E_h \text{ s.t.} \\ J(u_h) = \min\limits_{v_h \in E_h} J(v_h). \end{cases} \tag{2.7}$$

The main result of this paper is stated in the following theorem.

THEOREM 2.1. (i) *Problem* (2.7) *has at least one global minimizer.*

(ii) *There are no local minimizers.*

(iii) *All minimizers satisfy the following stability property:*

$$\|u_h\|_E \lesssim \|f\|_F. \tag{2.8}$$

(iv) *All minimizers satisfy the a priori error bound*

$$\|u - u_h\|_E \lesssim \min_{v_h \in E_h} \|u - v_h\|_E, \tag{2.9}$$

and the following a posteriori error estimate holds:

$$\|u - u_h\|_E \lesssim \|f - Lu_h\|_F. \tag{2.10}$$

Proof. (i) Let $K_h \subset E_h$ be the ball of radius $\frac{2}{\alpha}\|f\|_F$ centered at 0. It is clear that

$$\inf_{v_h \in E_h} J((v_h) = \min\left(\inf_{v_h \in E_h \setminus K_h} J(v_h), \inf_{v_h \in K_h} J(v_h)\right).$$

But for all $v_h \in E_h \setminus K_h$ (i.e., $\|v_h\|_E > \frac{2}{\alpha}\|f\|_F$) we have

$$\begin{aligned} J(v_h) &\geq \|Lv_h\|_F - \|f\|_F \\ &\geq \alpha\|v_h\|_E - \|f\|_F \\ &> \|f\|_F \\ &> J(0), \end{aligned}$$

where we have used the stability condition (2.1). Since $0 \in K_h$, we infer that

$$\inf_{v_h \in E_h \setminus K_h} J(v_h) > J(0) \geq \inf_{v_h \in K_h} J(v_h).$$

That is to say,

$$\inf_{v_h \in E_h} J(v_h) = \inf_{v_h \in K_h} J(v_h).$$

As a result, the existence of a global minimizer is a simple consequence of the fact that J is continuous and K_h is compact (since E_h is finite-dimensional).

(ii) The functional $J(v_h) = \|Lu_h - f\|_F$ is obviously convex; hence, local minimizers of (2.7) are necessarily global.

(iii) From (i) we infer that any minimizer u_h is in K_h; hence, $\|u_h\|_E \lesssim \|f\|_F$.

(iv) The stability condition (2.1) yields

$$\begin{aligned} \alpha\|u - u_h\|_E &\leq \|Lu - Lu_h\|_F \\ &= \|f - Lu_h\|_F \\ &= \min_{v_h \in E_h} \|f - Lv_h\|_F \\ &= \min_{v_h \in E_h} \|Lu - Lv_h\|_F \\ &\leq \|L\|_{\mathcal{L}(E;F)} \min_{v_h \in E_h} \|u - v_h\|_E. \end{aligned}$$

The proof is complete. ∎

Remark 2.1. Note that the question of the uniqueness of u_h is open. Actually, it may happen that u_h is not unique. To gain some insight on this problem, let us consider $D = \{(x_1, x_2) \in \mathbb{R}^2 \,|\, x_1 + x_2 \geq 1\}$, $x_0 = (0, 0)$, and let us define S to be the set of points in D that minimize the ℓ^1-distance to x_0. A simple calculation shows $S = \{(x_1, x_2) \in \mathbb{R}^2 \,|\, x_1 + x_2 = 1,\, x_1 \geq 0,\, x_2 \geq 0\}$; that is, even though the functional and D are convex, the solution to this minimization problem is not unique. Of course, uniqueness would have been guaranteed if we had considered the Euclidean (Hilbertian) distance.

Now, using a standard density argument, we deduce the following corollary.

COROLLARY 2.1. *Under the hypotheses of Theorem* 2.1 *and* (2.6) *we have*

$$\lim_{h \to 0} \|u - u_h\|_E = 0, \tag{2.11}$$

and if $u \in W$*, the following a priori error estimate holds:*

$$\|u - u_h\|_E \lesssim \epsilon(h)\|u\|_W. \tag{2.12}$$

Remark 2.2.

(i) Note that the a priori error estimate (2.12) is optimal since it is bounded by the interpolation error up to a constant.

(ii) Note that the price paid for the approximation optimality when $F = L^1(\Omega)$ is the loss of differentiability. More precisely, the functional $J(v_h) = \|Lu_h - f\|_{L^1(\Omega)}$ is not differentiable; hence, no first-order optimality condition can be written. To better appreciate the difficulty we face here, think of the following two functionals: $\phi(x) = x^2$ and $\psi(x) = |x|$. It is clear that the minimum of ϕ is reached at x_0 when $\phi'(x_0) = 2x_0 = 0$, whereas no nice first-order optimality condition can be written for ψ except for the awkward statement that 0 is in the subdifferential of $\psi(x_0)$, i.e., $0 \in \partial\psi(x_0)$. We describe an algorithm in section 3.6 to solve this difficulty. ∎

3. The $L^p(\Omega)$ setting. We show in this section how the above abstract result can be reformulated in the $L^p(\Omega)$ setting for first-order PDEs.

3.1. Formulation of the problem. In the context of first-order PDEs, F is usually a space $L^p(\Omega)^m$, $1 \le p < \infty$ (or possibly a closed subspace of $L^p(\Omega)^m$), and E is the domain of an unbounded linear operator

$$L : D(L) = E \subset L^p(\Omega)^m \longrightarrow L^p(\Omega)^m = F$$

whose graph is closed in $L^p(\Omega)^m \times L^p(\Omega)^m$ and whose domain $D(L)$ is dense in $L^p(\Omega)^m$ so that when the vector space $E = D(L)$ is equipped with the graph norm $\|v\|_E = (\|v\|^p_{L^p(\Omega)^m} + \|Lv\|^p_{L^p(\Omega)^m})^{\frac{1}{p}}$ it becomes a Banach space.

In this setting, the abstract problem (2.3) is interpreted as follows: For $f \in L^p(\Omega)^m$,

$$\begin{cases} \text{find } u \in E \text{ s.t.} \\ Lu = f \quad \text{ in } L^p(\Omega)^m. \end{cases} \tag{3.1}$$

Owing to the Riesz representation theorem, which permits us to identify the dual of $L^p(\Omega)^m$ with $L^{p'}(\Omega)^m$, where $\frac{1}{p} + \frac{1}{p'} = 1$, this problem can be alternatively put into the following form:

$$\begin{cases} \text{Find } u \in E \text{ s.t.} \\ \displaystyle\int_\Omega \phi \cdot Lu = \int_\Omega f \cdot \phi \quad \forall \phi \in L^{p'}(\Omega)^m. \end{cases} \tag{3.2}$$

3.1.1. Example 1: Advection-reaction. Let us consider an advection-reaction problem. Let $\boldsymbol{\beta}$ be a smooth vector field in $\mathbb{R}^d$, say $\boldsymbol{\beta} \in L^\infty(\Omega)^d$ and $\nabla\cdot\boldsymbol{\beta} \in L^\infty(\Omega)$, and set

$$\partial\Omega^- = \{x \in \partial\Omega \mid \boldsymbol{\beta}(x) \cdot \mathbf{n}(\mathbf{x}) < \mathbf{0}\},$$
$$\partial\Omega^+ = \{x \in \partial\Omega \mid \boldsymbol{\beta}(x) \cdot \mathbf{n}(\mathbf{x}) > \mathbf{0}\}.$$

$\partial\Omega^-$ is the inflow boundary, $\partial\Omega^+$ is the outflow boundary, and $\mathbf{n}(\mathbf{x})$ is the unit exterior normal to $\partial\Omega$ at $x \in \partial\Omega$. It may happen that these two subsets of $\partial\Omega$ are empty if $\boldsymbol{\beta}$ is s.t. $\boldsymbol{\beta} \cdot \mathbf{n}(\mathbf{x}) = \mathbf{0}$ for all $x \in \partial\Omega$. Let μ be a function in $L^\infty(\Omega)$, and assume that there is a constant $\mu_0 > 0$ so that

$$\mu(x) \ge \mu_0 > 0 \quad \text{a.e. } x \text{ in } \Omega. \tag{3.3}$$

We introduce the differential operator

$$L(u) = \mu u + \nabla\cdot(u\boldsymbol{\beta}),$$

with domain

$$E = D(L) = \{w \in L^1(\Omega);\ \nabla\cdot(w\boldsymbol{\beta}) \in L^1(\Omega);\ \boldsymbol{\beta}\cdot\mathbf{n}|_{\partial\Omega^-} = 0\} \subset L^1(\Omega) = F.$$

It can be shown that L is an isomorphism from E to F; i.e., (2.1) and (2.2) hold.

Remark 3.1. If $\mu = 0$, the hypothesis (3.3) is not satisfied. Nevertheless, L is still an isomorphism if $\boldsymbol{\beta}$ is a smooth filling field, i.e., if for almost every x in Ω there is a characteristic of $\boldsymbol{\beta}$ that starts from x and reaches $\partial\Omega^-$ in finite time. The reader is referred to Azerad and Pousin [1] for other details on this problem.

3.1.2. Example 2: The Darcy equation. Let Ω be a porous medium characterized by the permeability tensor $\mathbf{K}(\mathbf{x})$. This tensor is assumed to be symmetric positive definite, and its smallest and largest eigenvalues are assumed to be bounded from below and from above uniformly in Ω. We consider the following problem:

$$\begin{cases} \mathbf{K^{-1}}\cdot\mathbf{u} + \nabla\mathbf{p} = \mathbf{f}, \\ \nabla\cdot\mathbf{u} + \alpha\mathbf{p} = \mathbf{g}, \\ p_{|\partial\Omega} = 0. \end{cases} \tag{3.4}$$

This problem is known as the Darcy problem. It is also the mixed form of the Poisson problem. Nonlinear versions of (3.4) play important roles in underground storage problems, hydrogeology, and the petroleum industry. It is very often coupled with a transport equation for the concentration of a chemical species or a phase fraction.

To formulate (3.4) in the $L^p(\Omega)$ setting, we introduce some definitions:

$$\begin{aligned} X &= \{\mathbf{v} \in \mathbf{L^p(\Omega)^d};\ \nabla\cdot\mathbf{v} \in \mathbf{L^p(\Omega)}\}, \\ \|\mathbf{v}\|_{\mathbf{X}} &= (\|\mathbf{v}\|^{\mathbf{p}}_{\mathbf{L^p(\Omega)^d}} + \|\nabla\cdot\mathbf{v}\|^{\mathbf{p}}_{\mathbf{L^p(\Omega)}})^{\frac{1}{\mathbf{p}}}, \\ Y &= \{q \in L^p(\Omega);\ \nabla q \in L^p(\Omega)^d,\ q_{|\partial\Omega} = 0\}, \\ \|q\|_Y &= \|q\|_{W^{1,p}(\Omega)} = (\|q\|^p_{L^p(\Omega)} + \|\nabla q\|^p_{L^p(\Omega)^d})^{\frac{1}{p}}. \end{aligned}$$

X and Y are Banach spaces. We set $E = X \times Y$ and $F = L^p(\Omega)^d \times L^p(\Omega)$, which we equip with the norms $\|(\mathbf{v},\mathbf{q})\|_{\mathbf{E}} = (\|\mathbf{v}\|^{\mathbf{p}}_{\mathbf{X}} + \|\mathbf{q}\|^{\mathbf{p}}_{\mathbf{Y}})^{\frac{1}{\mathbf{p}}}$ and $\|(\mathbf{v},\mathbf{q})\|_{\mathbf{F}} = (\|\mathbf{v}\|^{\mathbf{p}}_{\mathbf{L^p(\Omega)^d}} + \|\mathbf{q}\|^{\mathbf{p}}_{\mathbf{L^p(\Omega)}})^{\frac{1}{\mathbf{p}}}$, respectively. We now define the operator

$$\begin{aligned} &L : E \longrightarrow F, \\ &(\mathbf{v},\mathbf{q}) \longmapsto (\mathbf{K^{-1}}\mathbf{v} + \nabla\mathbf{q}, \nabla\cdot\mathbf{v} + \alpha\mathbf{q}). \end{aligned}$$

L is clearly continuous, and it can be shown that it is an isomorphism if $\alpha \geq 0$, for $1 < p < +\infty$, and if $\alpha > 0$ for $p = 1$ (see, e.g., [6, 11, 34]).

3.2. Friedrichs's systems. The above two examples are particular cases of Friedrichs's symmetric systems; see [19]. Most of what is said hereafter generalizes to this broad class of PDEs.

3.3. The discrete setting. Henceforth, we assume that F is a closed subspace of $L^p(\Omega)^m$. We assume also that we are given a sequence of regular finite element meshes $(\mathcal{T}_h)_{h>0}$ covering the domain Ω. With each mesh we associate a finite-dimensional space $E_h \subset E$ having some interpolation properties; that is, there is a dense normed subspace of smooth functions $W \subset E$ and a continuous function $\epsilon(h)$ with $\epsilon(0) = 0$ s.t. (2.6) holds. For $\mathbb{P}_k$ or $\mathbb{Q}_k$ Lagrange finite elements, we have $\epsilon(h) = h^k$, where h is the meshsize.

3.4. A brief review of some standard techniques. One of the standard ways of approximating (3.2) without invoking a minimization principle like (2.7) is the Galerkin technique. This method consists in replacing the solution space, E, and the test space, $L^{p'}(\Omega)^m$, by the same discrete space E_h as follows:

$$\begin{cases} \text{Find } u_h \in E_h \text{ s.t.} \\ \displaystyle\int_\Omega \phi_h \cdot Lu_h = \int_\Omega \phi_h \cdot f \quad \forall \phi_h \in E_h. \end{cases} \tag{3.5}$$

Note that using the same space for testing the equation and approximating the solution guarantees that the corresponding linear system has as many equations as unknowns. Even though it often happens that the discrete solution is unique, (3.5) does not yield stability in the E-norm in general. To better appreciate this point, let us consider the scalar problem $u' = f$ with $u(0) = 0$ in the one-dimensional (1D) domain $\Omega =]0,1[$, where we assume $f \in L^2(\Omega)$. For $N \in \mathbb{N}^\star$, let us set $h = 1/N$ and $x_i = ih$ for $i \in \{0, 1, \ldots, N\}$. We define

$$E_h = \{v_h \in \mathcal{C}^0(\overline{\Omega});\ v_{h|[x_i,x_{i+1}]} \in \mathbb{P}_1,\ 0 \le i \le N-1;\ v_h(0) = 0\}. \tag{3.6}$$

It is clear that $E_h \subset E = \{v \in H^1(\Omega);\ v(0) = 0\}$. The discrete Galerkin formulation of the problem is as follows:

$$\begin{cases} \text{Find } u_h \text{ in } E_h \text{ s.t.} \\ \displaystyle\int_0^1 v_h u_h' = \int_0^1 v_h f \qquad \forall v_h \in E_h, \end{cases} \tag{3.7}$$

and its stability constant (i.e., the counterpart of α in (2.1)) is

$$\alpha_h := \inf_{u_h \in E_h} \sup_{v_h \in E_h} \frac{\int_0^1 u_h' v_h}{\|u_h\|_{H^1(\Omega)} \|v_h\|_{L^2(\Omega)}}.$$

The following negative result can be proved.

THEOREM 3.1. *There are two constants $c_1 > 0$ and $c_2 > 0$, independent of h, s.t.*

$$c_1 h \le \alpha_h \le c_2 h.$$

Proof. See, e.g., Ern and Guermond [18, pp. 197–199]. ∎

In other words, the stability constant for the approximate problem (3.7) goes to zero as the mesh is refined. This result is the main reason for the failure of the Galerkin technique to work properly for first-order PDEs in general.

An interesting alternative to the Galerkin formulation consists in the least-squares formulation. The origins of the least-squares technique can be traced back to Gauss (*Theoria Motus Corporum Coelestium* (1809)). As early papers in the numerical analysis literature we cite the series of papers by Bramble and Schatz [9, 10] published in 1970. Since then, it has been applied to a wide variety of problems (see, e.g., [2, 33, 24]). This method is clearly optimal in the $L^2(\Omega)$-graph norm, but it performs poorly when the source term is not in $L^2(\Omega)$ but in $L^1(\Omega)$ only or the boundary data are discontinuous (see the numerical tests in section 4).

The list of alternative techniques for solving (3.2) is quite long, and it is out of the question to make this list exhaustive, but among the most popular ones is the so-called Galerkin least-squares method [16, 25], which combines the accuracy of the Galerkin

method and the stability properties of the least-squares method. Other methods of interest are those based on discontinuous interpolation spaces (e.g., discontinuous Galerkin methods [31, 17]), on bubble functions (e.g., residual free bubble methods [13, 3, 14]), or on a hierarchical decomposition of the approximation space (e.g., subgrid stabilization [20, 21, 15] or spectral viscosity [35]). Although all these methods are quite efficient in general, they cannot cope with discontinuities and boundary layers without resorting to shock-capturing and nonlinear limiting techniques [26, 22] since they are all L^2-based; i.e., they rely on a priori L^2 estimates.

3.5. The discrete problem and regularization. Upon setting $J(v) = \|Lv - f\|_{L^p(\Omega)^m}$, the minimization problem we would like to solve is to find u_h in E_h such that $J(u_h) = \min_{v_h \in E_h} J(v_h)$. Actually, since $\mathbb{R}^+ \ni x \longmapsto x^p$ is an increasing function, an equivalent reformulation consists of setting

$$\mathcal{J}(v) = \|Lv - f\|^p_{L^p(\Omega)^m}$$

and considering the following problem:

$$\begin{cases} \text{Find } u_h \in E_h \text{ s.t.} \\ \mathcal{J}(u_h) = \min\limits_{v_h \in E_h} \mathcal{J}(v_h). \end{cases} \tag{3.8}$$

To handle this possibly nondifferentiable minimization problem by means of standard gradient techniques, we propose to regularize it as follows. Let us define $\varepsilon > 0$ and introduce

$$\varphi_\varepsilon(r) = r^2(r+\varepsilon)^{p-2}. \tag{3.9}$$

Then we regularize $\mathbb{R}^m \ni x \longmapsto \|x\|^p_{\ell^p}$ by replacing this function by

$$\psi_\varepsilon(x) = \sum_{i=1}^m \varphi_\varepsilon(|x_i|). \tag{3.10}$$

Upon denoting by $\mathrm{sg}(t)$ the sign function (i.e., $\mathrm{sg}(t) = t/|t|$ if $t \neq 0$ and $\mathrm{sg}(0) = 0$), we have

$$\forall v \in \mathbb{R}^m, \quad D\psi_\varepsilon(x) \cdot v = \sum_{i=1}^m \varphi'_\varepsilon(|x_i|)\mathrm{sg}(x_i)v_i, \tag{3.11}$$

$$\forall v, w \in \mathbb{R}^m, \quad w \cdot D^2\psi_\varepsilon(x) \cdot v = \sum_{i=1}^m \varphi''_\varepsilon(|x_i|)v_i w_i. \tag{3.12}$$

Note that φ''_ε is a decreasing function on $\mathbb{R}^+$ if $1 \le p \le 2$, and it is an increasing function if $p \ge 2$. More precisely, we have the following:

$$\text{if } 1 \le p \le 2, \quad \exists c > 0 \ \forall a > 0, \ \forall r \in [0,a], \quad c\,a^{p-2} \le \varphi''_\varepsilon(r) \le 2\,\varepsilon^{p-2}, \tag{3.13}$$

$$\text{if } 2 \le p, \quad \exists c > 0 \ \forall a > 0, \ \forall r \in [0,a], \quad 2\,\varepsilon^{p-2} \le \varphi''_\varepsilon(r) \le c\,a^{p-2}. \tag{3.14}$$

This, in turn, implies the following property:

$$\text{if } 1 \le p \le 2 \quad \begin{cases} \forall y \in \mathbb{R}^m, & c\,\|y\|^{p-2}_{\ell^\infty}\,\|y\|^2_{\ell^2} \le y \cdot D^2\psi_\varepsilon(x) \cdot y, \\ \forall y, z \in \mathbb{R}^m, & |z \cdot D^2\psi_\varepsilon(x) \cdot y| \le 2\,\varepsilon^{p-2}\,\|z\|_{\ell^2}\|y\|_{\ell^2}, \end{cases} \tag{3.15}$$

and an obvious similar property holds if $p \ge 2$.

Now we introduce the regularized functional

$$\mathcal{J}_\varepsilon(v_h) = \int_\Omega \psi_\varepsilon(Lu_h - f), \tag{3.16}$$

and we define u_h^ε to be a solution to the following minimization problem:

$$\begin{cases} \text{Find } u_h^\varepsilon \in E_h \text{ s.t.} \\ \mathcal{J}_\varepsilon(u_h^\varepsilon) = \min\limits_{v_h \in E_h} \mathcal{J}_\varepsilon(v_h). \end{cases} \tag{3.17}$$

It is clear that, owing to the regularization, $\mathcal{J}_\varepsilon$ is differentiable (in the Fréchet sense), and the first-order optimality condition for (3.17) is

$$\int_\Omega D\psi_\varepsilon(Lu_h^\varepsilon - f) \cdot Lv_h = 0 \quad \forall v_h \in E_h.$$

The algorithm that we propose in the next section consists in obtaining a solution to (3.8) as a limit of a sequence $(u_h^\varepsilon)_{\varepsilon>0}$ as $\varepsilon \to 0$.

Now we give a series of lemmas clarifying the stability of u_h^ε with respect to the data, the uniqueness of u_h^ε, the convergence of the sequence $(u_h^\varepsilon)_{\varepsilon>0}$ as $\varepsilon \to 0$, and, finally, the convergence of the sequence $(u_h^\varepsilon)_{\varepsilon>0,h>0}$ as both ε and h go to zero.

LEMMA 3.1. *Solutions to* (3.17) *satisfy the following stability estimate:*

$$\alpha \|u_h^\varepsilon\|_E \le \|f\|_{L^p(\Omega)^m} + (m\,\varepsilon^p|\Omega| + 2\|\psi_\varepsilon(f)\|_{L^1(\Omega)})^{\frac{1}{p}}.$$

Proof. Owing to the definition of φ_ε, it is clear that for all $g \in L^p(\Omega)^m$,

$$1 \le i \le m, \qquad \frac{1}{2}\int_{\{|g_i|\ge\varepsilon\}} |g_i|^p \le \int_\Omega \varphi_\varepsilon(|g_i|).$$

As a result,

$$\int_\Omega |g_i|^p = \int_{\{|g_i|<\varepsilon\}} |g_i|^p + \int_{\{|g_i|\ge\varepsilon\}} |g_i|^p \le \varepsilon^p|\Omega| + 2\int_\Omega \varphi_\varepsilon(|g_i|)$$

and

$$\int_\Omega \|g\|_{\ell^p}^p \le m\,\varepsilon^p|\Omega| + 2\int_\Omega \psi_\varepsilon(g).$$

Hence,

$$\int_\Omega \|Lu_h^\varepsilon - f\|_{\ell^p}^p \le m\,\varepsilon^p|\Omega| + 2\int_\Omega \psi_\varepsilon(Lu_h^\varepsilon - f) \le m\,\varepsilon^p|\Omega| + 2\int_\Omega \psi_\varepsilon(f).$$

The triangle inequality, together with (2.1), yields the result. ∎

LEMMA 3.2. *If $f \in L^\infty(\Omega)^m$, there is a unique function u_h^ε minimizing $\mathcal{J}_\varepsilon$.*

Proof. Let u_h^1 and u_h^2 be two functions in E_h. We have

$$\begin{aligned} D\mathcal{J}_\varepsilon(u_h^1)(v_h) - D\mathcal{J}_\varepsilon(u_h^2)(v_h) &= \int_\Omega [D\psi_\varepsilon(Lu_h^1 - f) - D\psi_\varepsilon(Lu_h^2 - f)] \cdot Lv_h \\ &= \int_\Omega L(u_h^1 - u_h^2) \cdot \int_0^1 D^2\psi_\varepsilon(R(s))ds \cdot Lv_h, \end{aligned}$$

where $R(s) = L(su_h^1 + (1-s)u_h^2) - f$. Now using $v_h = u_h^1 - u_h^2$ as a test function and making use of (3.15), we infer that

$$(D\mathcal{J}_\varepsilon(u_h^1) - D\mathcal{J}_\varepsilon(u_h^2))(u_h^1 - u_h^2) \geq \int_\Omega \alpha_\varepsilon(u_h^1, u_h^2, f)\|L(u_h^1 - u_h^2)\|_{\ell^2}^2,$$

where $\alpha_\varepsilon(u_h^1, u_h^2, f) = c \inf_{0\leq s\leq 1} \min(\|R(s)\|_{\ell^\infty}^{p-2})$ if $1 \leq p \leq 2$ and $\alpha_\varepsilon(u_h^1, u_h^2, f) = 2\varepsilon^{p-2}$ if $p \geq 2$.

If u_h^1 and u_h^2 both minimize $\mathcal{J}_\varepsilon$, then, owing to inverse inequalities, both of these functions are bounded. Since f is also assumed to be bounded, we necessarily have $\|Lu_h^i - f\|_{L^\infty(\Omega)^m} < +\infty$, $i = 1, 2$; that is to say, ess $\inf_\Omega \alpha_\varepsilon(u_h^1, u_h^2, f) > 0$ and

$$0 \geq \operatorname*{ess\,inf}_\Omega \alpha_\varepsilon(u_h^1, u_h^2, f) \int_\Omega \|L(u_h^1 - u_h^2)\|_{\ell^2}^2,$$

which yields $u_h^1 = u_h^2$ since L is injective. ∎

Since E_h is finite-dimensional (hence locally compact), a first consequence of Lemma 3.1 is that, up to a subsequence, $(u_h^\varepsilon)_{\varepsilon>0}$ converges to some u_h^0 in E_h.

LEMMA 3.3. *Every limit u_h^0 of $(u_h^\varepsilon)_{\varepsilon>0}$, up to a subsequence, is a solution to the unregularized minimization problem* (3.8).

Proof. First, let us observe that

$$\forall p \geq 1,\ \forall x \in \mathbb{R}, \qquad |\varphi_\varepsilon(|x|) - |x|^p| \leq (2+p)2^p\,\varepsilon\,(|x|^{p-1} + \varepsilon^{p-1}).$$

As a result, for all $x \in E$, we have

$$\begin{aligned}|\mathcal{J}_\varepsilon(x) - \mathcal{J}(x)| &\leq (2+p)2^p\,\varepsilon \int_\Omega \left(\sum_{i=1}^m |L_i x - f_i|^{p-1} + \varepsilon^{p-1}\right) \\ &\leq (2+p)2^p\,\varepsilon\,(m\,\varepsilon^{p-1}|\Omega| + m^{\frac{1}{p}}|\Omega|^{\frac{1}{p}}\mathcal{J}(x)^{\frac{p-1}{p}}).\end{aligned} \tag{3.18}$$

Furthermore, for all x^1 and x^2 in E, we have

$$|\mathcal{J}(x^1)^{\frac{1}{p}} - \mathcal{J}(x^2)^{\frac{1}{p}}| = |\|Lx^1 - f\|_F - \|Lx^2 - f\|_F| \leq \|L\|\,\|x^1 - x^2\|_E.$$

Combining these two results, we infer that if $x^\varepsilon \to x^0$ in E, then $\mathcal{J}_\varepsilon(x^\varepsilon) \to \mathcal{J}(x^0)$. Then we have

$$\mathcal{J}(u_h^0) = \lim_{\varepsilon\to 0} \mathcal{J}_\varepsilon(u_h^\varepsilon) = \lim_{\varepsilon\to 0} \min_{v_h\in E_h} \mathcal{J}_\varepsilon(v_h) = \min_{v_h\in E_h} \mathcal{J}(v_h),$$

which means that u_h^0 minimizes $\mathcal{J}$ in E_h. ∎

LEMMA 3.4. *Every solution to problem* (3.17) *is such that*

$$\|u - u_h^\varepsilon\|_E \lesssim \left(\varepsilon\,c(\|f\|_F) + \min_{v_h\in E_h} \|u - v_h\|_E^p\right)^{\frac{1}{p}},$$

where $c(\cdot)$ is a continuous function.

Proof. Owing to Lemma 3.1 and (3.18), we infer that

$$\begin{aligned}0 \leq \mathcal{J}(u_h^\varepsilon) - \mathcal{J}(u_h) &\leq \mathcal{J}(u_h^\varepsilon) - \mathcal{J}_\varepsilon(u_h^\varepsilon) + \mathcal{J}_\varepsilon(u_h^\varepsilon) - \mathcal{J}_\varepsilon(u_h) \\ &\quad + \mathcal{J}_\varepsilon(u_h) - \mathcal{J}(u_h) \\ &\leq \mathcal{J}(u_h^\varepsilon) - \mathcal{J}_\varepsilon(u_h^\varepsilon) + \mathcal{J}_\varepsilon(u_h) - \mathcal{J}(u_h) \\ &\lesssim \varepsilon\left(\varepsilon^{p-1} + \mathcal{J}(u_h^\varepsilon)^{\frac{p-1}{p}} + \mathcal{J}(u_h)^{\frac{p-1}{p}}\right) \\ &\lesssim \varepsilon\,c(\|f\|_F).\end{aligned}$$

Hence,

$$\begin{aligned}\|u-u_h^\varepsilon\|_E^p &\lesssim \|f-Lu_h^\varepsilon\|_F^p = \mathcal{J}(u_h^\varepsilon)-\mathcal{J}(u_h)+\mathcal{J}(u_h)\\ &\lesssim \varepsilon\, c(\|f\|_F)+\min_{v_h\in E_h}\|u-v_h\|_E^p.\end{aligned}$$

The proof is complete. ∎

Remark 3.2. Lemma 3.4 guarantees that if $\varepsilon^{1/p}$ is smaller than the interpolation error, then u_h^ε is as good an approximation of u as u_h. Note also that the smaller the p the smaller the error induced by regularization, and regularization is needed only if $1\le p<2$.

3.6. A simple algorithm for solving (3.8). We now present a simple algorithm for solving (3.8). The main idea is to set a sequence of regularization parameters $(\varepsilon^k)_{k\ge 0}$ tending to zero (or some numerically acceptable threshold) as k grows and then, for each parameter ε^k, to find a reasonable approximation of the minimizer of $\mathcal{J}_\varepsilon$ using Newton's algorithm and starting from the approximate minimizer evaluated at step $k-1$. More precisely, the algorithm we propose is as follows:

Step 1: Initialize ε^0 (say, $\varepsilon^0\sim h$) and compute some initial guess u_h^0 (use a crude $L^2(\Omega)$-stabilized technique; for instance, add a Laplace perturbation to the equation and evaluate the Galerkin solution, or evaluate the least-squares solution).

Step 2: Iterate on index k, starting from $k=0$.

Step 3$_k$: Set $u_h^{k,0}=u_h^k$.

Step 4$_k$: Iterate on index l, starting from $l=0$.

Step 5$_{k,l}$: Evaluate the gradient and the Hessian of $\mathcal{J}_{\varepsilon^k}(u_h^{k,l})$ as follows:

$$D\mathcal{J}_{\varepsilon^k}(u_h^{k,l})(v_h)=\int_\Omega D\psi_{\varepsilon^k}(Lu_h^{k,l}-f)\cdot Lv_h, \tag{3.19}$$

$$D^2\mathcal{J}_{\varepsilon^k}(u_h^{k,l})(v_h,w_h)=\int_\Omega Lw_h\cdot D^2\psi_{\varepsilon^k}(Lu_h^{k,l}-f)\cdot Lv_h. \tag{3.20}$$

Step 6$_{k,l}$: Deduce a descent direction, d_h, by solving the following problem:

$$\begin{cases}\text{Find } d_h\in X_h \text{ s.t.}\\ D^2\mathcal{J}_{\varepsilon^k}(u_h^{k,l})(v_h,d_h)=D\mathcal{J}_{\varepsilon^k}(u_h^{k,l})(v_h)\quad \forall v_h\in X_h.\end{cases} \tag{3.21}$$

Note that $D^2\psi_{\varepsilon^k}>0$; hence, in addition to being symmetric, the bilinear form $D^2\mathcal{J}_{\varepsilon^k}(u_h^{k,l})(v_h,w_h)$ is always positive definite; that is, (3.21) has always a unique solution.

Step 7$_{k,l}$: Make a line search of the minimum of $\mathcal{J}$ along the direction d_h. Call the corresponding solution $u_h^{k,l+1}$.

Step 8$_{k,l}$: If $\|u_h^{k,l+1}-u_h^{k,l}\|_E^p$ is smaller than ε^k, set $u_h^{k+1}=u_h^{k,l+1}$ and exit the l loop; otherwise continue iterations on l.

Step 9$_k$: If ε^k is smaller than some fixed tolerance, exit the k loop; otherwise divide ε^k by some fixed constant, say $\frac{3}{2}$, call the result ε^{k+1}, and continue iterations on k.

Step 10: Stop.

Remark 3.3.

(i) Note that at Step 7 the line search minimizes $\mathcal{J}$; hence, the algorithm always makes $\mathcal{J}$ decrease.

(ii) Note that in the above algorithm ε is not a tunable coefficient; i.e., this coefficient cannot be compared to any stabilizing parameter usually introduced by L^2-based stabilizing techniques (e.g., GaLS, residual free bubbles, subgrid viscosity, etc.). The sequence $(\varepsilon^k)_{k\geq 0}$ is meant to accelerate the convergence process, and it goes to zero as the number of iterations grows.

(iii) Note that the cost of one loop of the algorithm above is that of evaluating the Hessian and solving for the descent direction; however, (3.21) does not need to be solved very accurately. The computational cost per loop is identical to that of an approximate Galerkin solve. Hence, the total cost of the algorithm is that of an approximate Galerkin solve times the number of loops. In the examples reported below, the number of loops required to reach a reasonable convergence criterion was between 10 to 25 when using $u_h^0 = 0$. It is very likely that this crude algorithm is not optimal, and further research is needed to improve on this aspect of the problem. One can imagine, for instance, embedding the above algorithm within a multigrid strategy and/or some adaptive refinement strategy.

(iv) Using a stabilized L^2-based technique to compute u_h^0 significantly shortens the number of iterations in the above algorithm. In this context minimizing the residual in L^1 could be viewed as postprocessing for the L^2-based method.

(v) The above regularization-based iterative algorithm has some similarities with the so-called iteratively reweighted least-squares method of Jiang [24, Chap. 9].

(vi) When the operator L is nonlinear, the above algorithm still holds, provided formulas (3.19) and (3.20) defining the gradient and the Hessian of $\mathcal{J}_{\varepsilon^k}(u_h^{k,l})$ are modified accordingly. In this context, solving the problem in any $L^p(\Omega)$ does not cost more than solving the problem in the standard $L^2(\Omega)$ setting.

4. Numerical results. We report in this section on results of numerical tests meant to assess the theoretical a priori error estimates derived above and to illustrate the performance of the method when dealing with nonsmooth data and nonlinear problems. Unless stated explicitly otherwise, all the numerical tests reported herein have been performed in $L^1(\Omega)$.

4.1. Convergence tests.

4.1.1. A transport equation. We consider the two-dimensional (2D) domain $\Omega =]0,1[^2$ and the transport equation

$$\partial_x u = f, \quad u|_{x=0} = u_0, \tag{4.1}$$

with smooth data

$$f(x,y) = 2\pi\cos(2\pi(x+y)), \quad u_0(y) = \sin(2\pi y),$$

s.t. the exact solution is

$$u = \sin(2\pi(x+y)).$$

We approximate the solution using piecewise linear and piecewise quadratic triangular elements on unstructured Delaunay meshes. We compute the approximate solution of (4.1) in $L^1(\Omega)$. For the $\mathbb{P}_1$ solution we use meshes s.t. $\frac{1}{10} \leq h \leq \frac{1}{100}$, and for the $\mathbb{P}_2$ solution we take h in the range $\frac{1}{5} \leq h \leq \frac{1}{60}$. All the integrals are evaluated by using the 3 Gauss points quadrature rule for the $\mathbb{P}_1$ solution and the 7 Gauss points

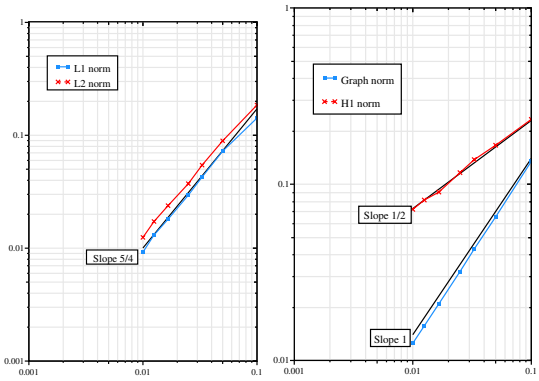

FIG. 1. *Convergence tests for $\mathbb{P}_1$ approximation. Left: Error in the L^1-norm and L^2-norm vs. the meshsize. Right: Error in the $L^1(\Omega)$-graph norm and H^1-norm vs. the meshsize.*

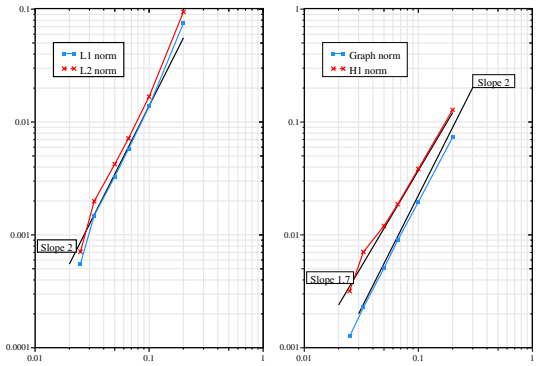

FIG. 2. *Convergence tests for $\mathbb{P}_2$ approximation. Left: Error in the L^1-norm and L^2-norm vs. the meshsize. Right: Error in the $L^1(\Omega)$-graph norm and H^1-norm vs. the meshsize.*

quadrature rule for the $\mathbb{P}_2$ solution. We evaluate the errors in the L^1-norm, the L^2-norm, the $L^1(\Omega)$-graph norm, and the H^1-norm. The results for the $\mathbb{P}_1$ approximation are displayed in Figure 1, and those for the $\mathbb{P}_2$ approximation are shown in Figure 2.

We note that the a priori error estimate (2.12) in the $L^1(\Omega)$-graph norm is fully confirmed: the slope is of order one with $\mathbb{P}_1$ finite elements and of order two with $\mathbb{P}_2$ finite elements. The error in the H^1-norm is of order $\frac{1}{2}$ for the $\mathbb{P}_1$ approximation and of order 1.7 for the $\mathbb{P}_2$ approximation. The fact that the convergence orders in the $L^1(\Omega)$-graph norm and the H^1-norm are different confirms that the method performs as expected and that it does not introduce excessive artificial cross-wind diffusion. The convergence rates of the error in the L^1-norm and the $L^2(\Omega)$-norm are slightly better than first-order in the $\mathbb{P}_1$ case and better than second-order in the $\mathbb{P}_2$ case. Note, however, that in both cases the rates are suboptimal. This result is not surprising since transport equations have no regularizing effects; that is, the Nitsche–Aubin duality argument that holds for elliptic equations does not hold here.

4.2. An elliptic operator. We now test the method on the Laplace operator. We use again $\Omega =]0,1[^2$. We solve

$$-\nabla^2 p = f, \quad p|_{\partial\Omega} = p_0,$$

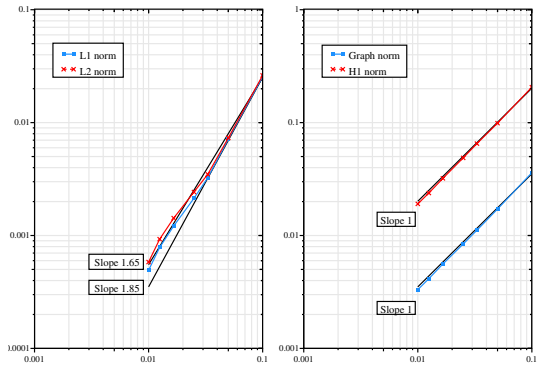

FIG. 3. *Convergence tests for $\mathbb{P}_1$ approximation of the Laplace operator. Left: Error in the L^1-norm and L^2-norm vs. the meshsize. Right: Error in the $L^1(\Omega)$-graph norm and H^1-norm vs. the meshsize.*

with the data being s.t. $p = x + 2y + \sin(2\pi x)\cos(2\pi y)$ is the exact solution.

The problem is rewritten in its first-order form (3.4) and solved in this form. We approximate the solution in $L^1(\Omega)$ using $\mathbb{P}_1$ finite elements on unstructured Delaunay meshes with $\frac{1}{10} \leq h \leq \frac{1}{100}$. For each mesh we measure the error in the $L^1(\Omega)$-norm, the $L^2(\Omega)$-norm, the $W^{1,1}(\Omega)$-norm, and the $H^1(\Omega)$-norm. The results are reported in Figure 3. We observe that the rate of convergence in the $W^{1,1}(\Omega)$-norm and in the $H^1(\Omega)$-norm are of first order; that is, they are optimal. Note that the error in the $W^{1,1}(\Omega)$-norm is almost eight times lower than that in the $H^1(\Omega)$-norm. For the $L^1(\Omega)$-norm there is not a clear rate, but we observe that the numerical results are bracketed by two lines of slope 1.65 and 1.85. Hence, the convergence is not second-order, but it is close to second-order. A similar conclusion holds for the convergence rate in the $L^2(\Omega)$-norm.

4.3. Transport equation with shock-like solutions. To illustrate the performance of the method when dealing with nonsmooth data, we consider again the 2D rectangular domain $\Omega =]0,1[^2$, and we solve the transport equation

$$\partial_x u = f, \quad u|_{x=0} = u_0, \tag{4.2}$$

with the two source terms

$$f_1(x,y) = \tfrac{1}{2\gamma}\Big[1 - \tanh^2\big(\tfrac{x-0.5}{\gamma}\big)\Big],$$
$$f_2(x,y) = \tfrac{1}{2\gamma}\Big[1 - \tanh^2\big(\tfrac{x-0.5(y+0.5)}{\gamma}\big)\Big],$$

for which the respective solutions are

$$u_1(x,y) = \tfrac{1}{2}\Big[1 + \tanh\big(\tfrac{x-0.5}{\gamma}\big)\Big],$$
$$u_2(x,y) = \tfrac{1}{2}\Big[1 + \tanh\big(\tfrac{x-0.5(y+0.5)}{\gamma}\big)\Big],$$

where $\gamma > 0$ is a small parameter. The source terms f_1 and f_2 are approximations of Dirac measures supported by the segments $x = \frac{1}{2}$ and $x - \frac{1}{2}(y - \frac{1}{2})$, respectively. These data mimic shock-like solutions.

To emphasize the capability of the method to perform well on unrefined and unstructured meshes, we show in Figure 4 the approximate solutions calculated on a

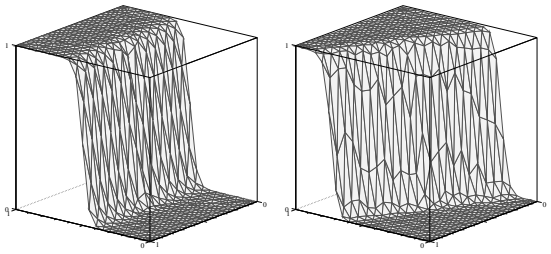

FIG. 4. *Piecewise linear L^1 approximations for test cases* (4.2). *Left: source term f_1; right: source term f_2.*

Delaunay mesh composed of 932 triangles of meshsize $h = \frac{1}{20}$. The parameter γ in the definition of the source terms is chosen to be $\gamma = h$ to guarantee that the inexact numerical integrations of the residuals are accurate enough.

Note that the solutions do not exhibit spurious over- or undershootings.

4.4. Transport equation with shear-layer-like solutions. In this section, we compare the performance of the method with that of the least-squares method on a transport equation with discontinuous boundary data.

4.4.1. 1D transport. We consider the 2D rectangular domain

$$\Omega =]0.2, 0.8[\times]0, 2[,$$

and we solve the following transport equation:

$$\partial_x u = 0, \quad u|_{x=0} = \begin{cases} 1 & \text{if } y \geq 0.5, \\ 0 & \text{otherwise.} \end{cases} \tag{4.3}$$

The exact solution is

$$u(x, y) = \begin{cases} 1 & \text{if } y \geq 0.5, \\ 0 & \text{otherwise.} \end{cases}$$

We perform the calculations on a Delaunay mesh with $h = \frac{1}{40}$. Due to the interpolation process, the boundary data is regularized for $0.475 \leq y \leq 0.525$.

We evaluate the least-squares solution (i.e., the $L^2(\Omega)$ approximation) and the $L^1(\Omega)$ approximation. The results are shown in Figure 5. The $L^1(\Omega)$ solution is shown at the top of the figure, and the $L^2(\Omega)$ one is shown at the bottom. For each solution we show contour lines in the left panels of the figure. Note that for both solutions there is some smearing in the transverse direction at the onset of the flow. This is due to the fact that the mesh is not aligned with the flow and the boundary data has been interpolated. In the right panels we show the projection of the graph of each solution onto the plane $x = 0$. It is clear that the least-squares solution is significantly more smeared than the $L^1(\Omega)$ one. The least-squares solution also exhibits over- and undershootings; i.e., it does not satisfy the maximum principle.

4.4.2. Curved transport. We consider the half disk

$$\Omega = \{(x, y);\ \sqrt{x^2 + y^2} < 1;\ y > 0\},$$

and let us set $\partial\Omega^- = \{-1 < x < 0;\ y = 0\}$. We want to solve the following transport problem:

$$\mathbf{v} \cdot \nabla u = 0, \quad u|_{\partial\Omega^-} = \begin{cases} 1 & \text{if } -1 < x < -0.74, \\ 0 & \text{if } -0.74 < x < 0, \end{cases} \tag{4.4}$$

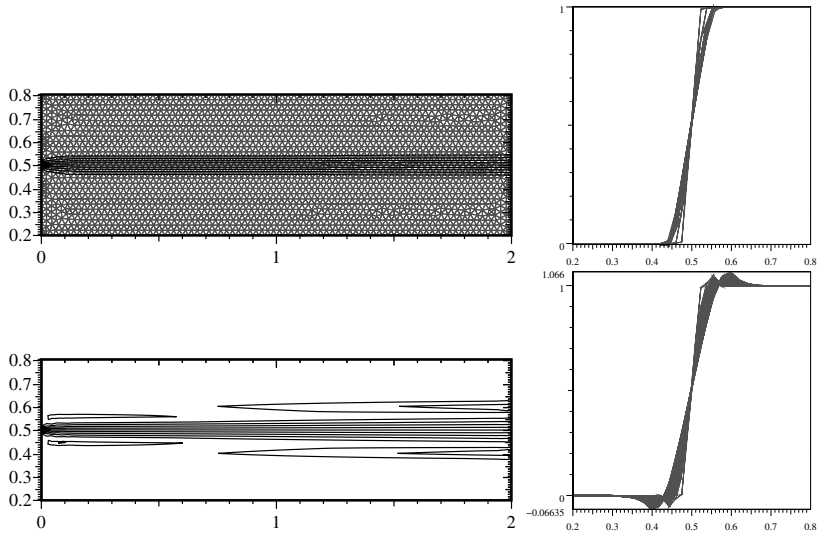

FIG. 5. *Advection equation* (4.3). *Top:* $L^1(\Omega)$ *solution and mesh; bottom:* $L^2(\Omega)$ *solution.*

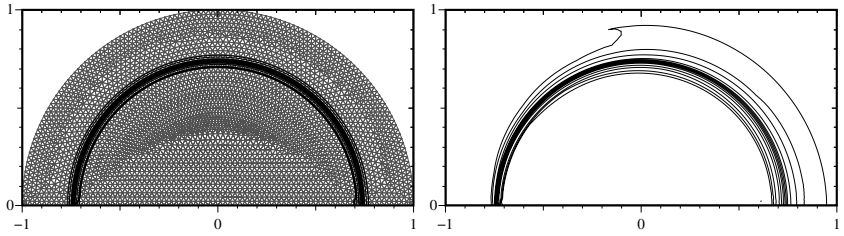

FIG. 6. *Advection equation* (4.4). *Left:* $L^1(\Omega)$ *solution with mesh; right:* $L^2(\Omega)$ *solution.*

with the curved flow field $\mathbf{v}(\mathbf{x}, \mathbf{y}) = (\sin\theta, -\cos\theta)$, where θ is the polar angle; i.e., $\theta = \arctan(y/x) \in [0, \pi[$ with the convention $\arctan(\pm\infty) = \pi/2$. The exact solution is

$$u(x, y) = \begin{cases} 1 & \text{if } \sqrt{x^2 + y^2} > 0.74, \\ 0 & \text{otherwise.} \end{cases}$$

We perform the calculations on a Delaunay mesh with $h = \frac{1}{40}$. Due to the interpolation process, the boundary condition is regularized for $-0.765 \le x \le -0.715$.

Contour lines of the $L^1(\Omega)$ and $L^2(\Omega)$ solutions are shown in Figure 6. We show about 13 contour lines for each solution. The $L^1(\Omega)$ solution is shown in the left panel of the figure, and the $L^2(\Omega)$ one is shown in the right panel. For both solutions there is some smearing in the transverse direction at the onset of the flow due to misalignment of the flow with the mesh and the interpolation of the data. It is clear, once again, that the least-squares solution is significantly more smeared than the $L^1(\Omega)$ solution and exhibits over- and undershootings.

Remark 4.1. The two test cases considered above show that for a given mesh the $L^1(\Omega)$ solution has better qualitative properties than the standard $L^2(\Omega)$ solution. In particular, discontinuities are less smeared by the L^1 approximation technique. We observe also that the $L^1(\Omega)$ solution satisfies the maximum principle. This numerical observation has yet to be fully explained mathematically.

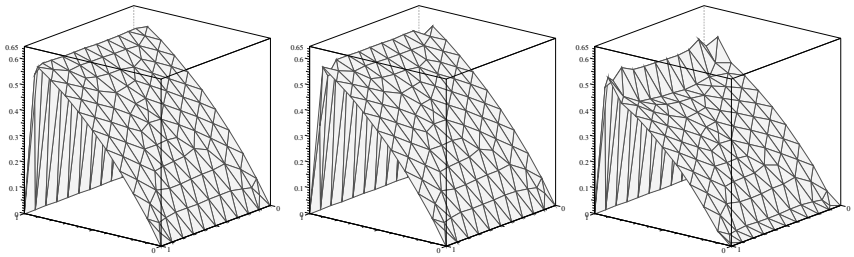

FIG. 7. *Advection equation* (4.5)*, Case* 1*,* $\nu = 0.02$*. Left:* $\mathbb{P}_1$ *Lagrange interpolate of the exact solution; center,* $L^1(\Omega)$ *solution; right,* $L^2(\Omega)$ *solution.*

Remark 4.2. Of course, if the meshes are adapted to the flow, results much sharper than those shown here can be easily obtained. We do not show these results here, for our objective in the present paper is rather to compare the performance of the $L^1(\Omega)$ and $L^2(\Omega)$ methods on arbitrary meshes than to show that each method can produce sharp results on adapted meshes.

4.5. Advection-diffusion equation. We conclude this series of tests on linear equations by solving an advection-diffusion equation in the vanishing viscosity regime.

For the sake of simplicity, we consider again the rectangular domain $\Omega =]0,1[^2$, and we denote

$$\partial\Omega_D = \{(x,y) \in \partial\Omega;\ x = 0 \text{ or } x = 1\},$$
$$\partial\Omega_N = \{(x,y) \in \partial\Omega;\ y = 0 \text{ or } y = 1\}.$$

We want to solve

$$\begin{cases} \alpha p + \boldsymbol{\beta} \cdot \nabla p + \sqrt{\nu}\, \nabla \cdot \mathbf{u} = \mathbf{f}, \\ \sqrt{\nu}\, \nabla p + \mathbf{u} = \mathbf{0}, \\ p_{|\partial\Omega_D} = p_D, \quad \mathbf{u} \cdot \mathbf{n}_{|\partial\boldsymbol{\Omega}_\mathbf{N}} = \mathbf{0}. \end{cases} \tag{4.5}$$

We set $\boldsymbol{\beta} = (1,0)$ s.t. the exact solution can be evaluated exactly.

4.5.1. Case 1. $\boldsymbol{\alpha \neq 0}$**.** We set

$$\alpha = 1, \quad f = 1, \quad p_D = 0. \tag{4.6}$$

The exact solution is

$$p(x,y) = \tfrac{1}{\alpha} + \mu^+ e^{\lambda^+ x} + \mu^- e^{\lambda^- x},$$
$$\lambda^{\pm} = \tfrac{-1 \pm \sqrt{1+4\alpha\nu}}{-2\nu}, \quad \mu^+ = -\tfrac{1}{\alpha} \tfrac{e^{\lambda^-} - 1}{e^{\lambda^-} - e^{\lambda^+}}, \quad \mu^- = -\tfrac{1}{\alpha} \tfrac{e^{\lambda^+} - 1}{e^{\lambda^+} - e^{\lambda^-}}. \tag{4.7}$$

We choose $\nu = 0.02$. We compute the $L^1(\Omega)$ and the least-squares approximations on a coarse grid with $h = \frac{1}{10}$. To the best of our knowledge, no finite element method is capable of producing a reasonable approximation to this problem with these parameters ($|\boldsymbol{\beta}|h/\nu = 5$) without resorting to some stabilization and/or nonlinear limiting technique. The results are shown in Figure 7. The $\mathbb{P}_1$ Lagrange interpolate of the exact solution is shown in the leftmost panel of the figure, the L^1 solution is in the center panel, and the least-squares solution is in the rightmost panel.

It is clear that the least-squares solution is far from the exact solution, whereas the L^1 one is a good approximation, considering the very low number of degrees of freedom used.

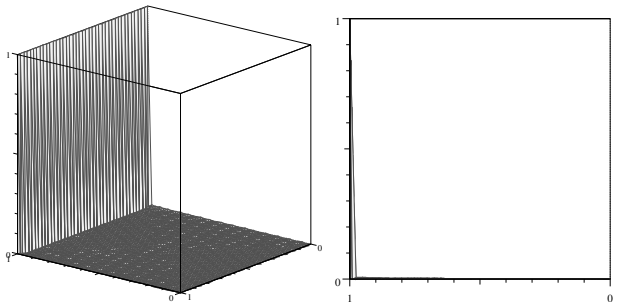

FIG. 8. *Advection equation* (4.5) *with* $\nu = 0.00125$, *Case* 2. *Left: side view of the graph of the approximate solution. Right: projection onto plane* $y = 0$ *of the graph of the approximate solution.*

4.5.2. Case 2. Now we set $\alpha = 0$. We choose the following data:

$$f = 0, \quad p_D = \begin{cases} 0 & \text{if } x = 0, \\ 1 & \text{if } x = 1. \end{cases} \tag{4.8}$$

The exact solution is

$$p(x, y) = \frac{e^{x/\nu} - 1}{e^{1/\nu} - 1}. \tag{4.9}$$

This case is frequently used in the literature to test the capability of numerical methods to solve advection-diffusion equations with dominant advection.

We set $\nu = 0.00125$, and we compute the $L^1(\Omega)$ solution on a grid of meshsize $h = \frac{1}{40}$. The result is shown in Figure 8.

It is clear that, within the capability of the mesh, the boundary layer is well-captured and the solution is not plagued by spurious oscillations.

4.6. Viscosity solutions of first-order PDEs. A striking property of the L^1 approximation technique is that it seemingly can select viscosity solutions of first-order PDEs (i.e., in the sense of Bardos, Leroux, and Nédélec [5] and Kružkov [27]).

4.6.1. Notion of viscosity solution. To illustrate this phenomenon, let Ω be a bounded domain of $\mathbb{R}^d$ with a smooth boundary. Let $\alpha > 0$, and let $\boldsymbol{\beta}$ be a vector field s.t. $\beta_i \in \mathcal{C}^1(\overline{\Omega})$, $1 \le i \le d$. Let u_0 be a smooth function on $\partial\Omega$, say $u_0 \in \mathcal{C}^2(\partial\Omega)$, and let $f \in W^{1,1}(\Omega)$. Following Bardos, Leroux, and Nédélec, [5], we say that u is a viscosity solution of

$$\alpha u + \nabla \cdot (\boldsymbol{\beta} u) = f, \quad u|_{\partial\Omega} = u_0, \tag{4.10}$$

if $u \in \mathrm{BV}(\Omega)$, u solves the PDE, and u satisfies the boundary condition in the following sense:

$$\int_{\partial\Omega} (\boldsymbol{\beta} \cdot \mathbf{n})(\mathbf{u} - \mathbf{k})(\mathrm{sg}(\mathbf{u} - \mathbf{k}) - \mathrm{sg}(\mathbf{u_0} - \mathbf{k})) \ge \mathbf{0} \quad \forall \mathbf{k} \in \mathbb{R}, \tag{4.11}$$

where $\mathrm{sg}(t)$ is the sign of t if $t \neq 0$ and $\mathrm{sg}(0) = 0$. In the present linear case, the boundary condition amounts to enforcing $u = u_0$ on $\partial\Omega^- = \{\mathbf{x} \in \partial\boldsymbol{\Omega} \,|\, \mathbf{x} \cdot \mathbf{n} < \mathbf{0}\}$. The interest of (4.11) is that it generalizes easily to nonlinear equations, whereas the notion of inflow and outflow boundary condition does not, since for nonlinear problems the inflow or outflow status of the boundary may depend on the solution

itself. For instance, if the linear term $\boldsymbol{\beta} u$ is replaced by $F(u, \mathbf{x})$, then the boundary condition $u|_{\partial\Omega} = u_0$ has to be understood in the sense

$$\int_{\partial\Omega} (F(u, \mathbf{x}) - \mathbf{F}(\mathbf{k}, \mathbf{x})) \cdot \mathbf{n}(\mathrm{sg}(\mathbf{u} - \mathbf{k}) - \mathrm{sg}(\mathbf{u_0} - \mathbf{k})) \geq \mathbf{0} \quad \forall \mathbf{k} \in \mathbb{R}. \tag{4.12}$$

Using arguments similar to those in [5] and [4], it is possible to prove that (4.10) has a unique viscosity solution, provided α is large enough. The bulk of the argument consists of proving that the solution to the following problem,

$$\alpha u_\epsilon + \nabla \cdot (\boldsymbol{\beta} u_\epsilon) - \epsilon \nabla^2 u_\epsilon = f, \quad u_\epsilon|_{\partial\Omega} = u_0, \tag{4.13}$$

converges in $\mathrm{BV}(\Omega)$ and the limit is the so-called viscosity solution; i.e., the limit satisfies the PDE in (4.10) and (4.11).

Despite the appearance, the problem (4.10) is not purely formal. It is typically this type of problem that arises when one tries to approximate (4.13) on meshes which are not refined enough. More precisely, when $\epsilon/h^2 \ll 1/h$ the second-order term in (4.13) is completely dominated by the first-order one, and solving (4.13) numerically amounts to trying to solve (4.10), where the boundary condition is understood in the classical sense instead of (4.11).

Once this point is understood, it becomes clear that the least-squares technique cannot work properly on the advection-diffusion equation (4.13) if the mesh is not refined enough.

PROPOSITION 4.1. *The H^1-conformal approximate least-squares solution to the linear problem* (4.13) *(written in mixed form) may not converge to the viscosity solution as $h \to 0$.*

Proof. As we want to build a counterexample, let us restrict ourselves to the 1D viewpoint, and let us take $\Omega =]0, 1[$, $\boldsymbol{\beta} = 1$, $u_0 = 0$, $\alpha = 1$, and $f = 1$. Let $E_h \subset H_0^1(\Omega)$ be a finite-dimensional finite element space. Thanks to crude a priori estimates in $L^2(\Omega)$ and standard inverse inequalities, it is clear that the least-squares approximation to (4.15) converges to the solution of the following problem as $\epsilon \to 0$:

$$\int_0^1 (u_h + u_h')(v_h + v_h') = \int_0^1 (v_h + v_h') \quad \forall v_h \in E_h.$$

Since test functions in E_h satisfy $v_h(0) = v_h(1) = 0$, we obtain

$$\int_0^1 (u_h + u_h')(v_h + v_h') = \int_0^1 v_h \quad \forall v_h \in E_h.$$

Then it is clear that, when $h \to 0$, the solution to the above problem converges in $H_0^1(]0, 1[)$ to the solution of the following PDE:

$$w - w'' = 1, \quad w(0) = w(1) = 0,$$

which is obviously different from the viscosity solution which solves

$$u + u' = 1, \quad u(0) = 0.$$

This completes the proof. ∎

This example shows that for a given mesh the L^2-based least-squares approximation technique does not select the right limit of (4.15) as $\epsilon \to 0$. The situation is quite different in $L^1(\Omega)$. For reasons not yet clear, numerical tests, reported in the next section, show that the solution that minimizes the L^1 distance is a reasonable approximation of the viscosity solution.

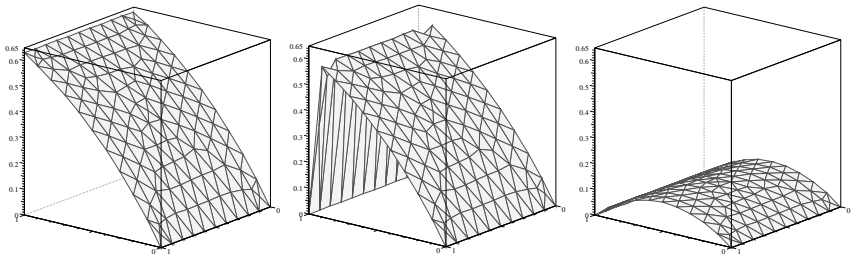

FIG. 9. *Viscosity solution to* (4.14). *Left:* $\mathbb{P}_1$ *Lagrange interpolate of the exact solution; center,* $L^1(\Omega)$ *solution; right,* $L^2(\Omega)$ *solution.*

4.6.2. Numerical experiments. let us consider the 2D rectangular domain $\Omega =]0,1[^2$ with $\partial\Omega_D = \{x = 0\} \cup \{x = 1\}$ and $\partial\Omega_N = \{y = 0\} \cup \{y = 1\}$. We want to solve the following scalar problem:

$$\alpha u + \partial_x u = f, \quad u|_{\partial\Omega_D} = u_0. \tag{4.14}$$

Of course, this problem is not well-posed in the standard sense since the outflow boundary condition is overspecified, but this problem is meaningful in the viscosity sense as defined above. Let E_h be a H^1-conformal finite element space s.t. for all v_h in E_h, $v_h|_{\partial\Omega_D} = 0$. It is clear that approximating the regularized problem

$$\alpha u_\epsilon + \partial_x u_\epsilon - \epsilon\nabla^2 u_\epsilon = f, \quad u_\epsilon|_{\partial\Omega_D} = u_0, \quad \partial_y u_\epsilon|_{\partial\Omega_N} = 0, \tag{4.15}$$

and taking the limit $\epsilon \to 0$, h being fixed, is equivalent to approximating (4.14) in E_h (recall that in E_h the Dirichlet boundary condition is enforced in the standard sense).

Let us set

$$\alpha = 1, \quad f = 1, \quad u_0 = 0. \tag{4.16}$$

We solve (4.14) in $L^1(\Omega)$ and in $L^2(\Omega)$, respectively, using continuous $\mathbb{P}_1$ finite elements and (3.8). To emphasize the capabilities of the L^1 approximation technique, we restrict ourselves to a very coarse mesh, $h = 1/10$. The results are shown in Figure 9.

In the left panel we show the $\mathbb{P}_1$ Lagrange interpolate of the viscosity solution, in the center panel we show the L^1 solution, and in the right panel we show the least-squares solution. Considering the mesh used, the $L^1(\Omega)$ approximation is a reasonable approximation, whereas the least-squares solution is completely wrong (thus confirming Proposition 4.1). Convergence tests, not reported here, show that the $L^1(\Omega)$ approximate solution converges in the $L^1(\Omega)$-norm to the viscosity solution as $h \to 0$.

Contrary to what it seems, the two horn-like spikes observable on the graph of the L^1 solution are not overshootings. These are perspective effects induced by the fact that the two corresponding $\mathbb{P}_1$-nodes are not aligned with the others. This is made clear by looking at the xz-projection of the graph of the L^1 solution shown in Figure 10.

Given that the least-squares method, together with its many variants, is a central part for the stabilization of the Galerkin technique (see, e.g., [16, 25, 26]), the above example gives new reasons why the Galerkin least-squares method cannot generally cope properly with shocks and boundary layers without the help of shock-capturing terms [26, 22].

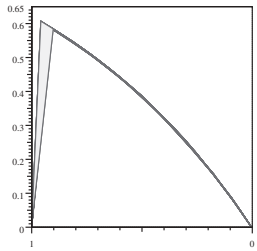

FIG. 10. *Projection in the xz-plane of the graph of the L^1 solutions in Figure 9.*

4.7. The Burgers equation. To finish this series of tests we propose to solve the Burgers-like equation

$$\nabla\cdot\left(\left(\boldsymbol{\beta}+\frac{u}{2}\frac{\mathbf{x}-\mathbf{x_0}}{\|\mathbf{x}-\mathbf{x_0}\|_{\ell^2}^{\mathbf{2}}}\right)u\right)=0,\quad u|_{\partial\Omega_1}=1,\quad u|_{\partial\Omega_0}=0, \tag{4.17}$$

in the following 2D domain:

$$\Omega=]0,1[^2\setminus\{\|\mathbf{x_0}-\mathbf{x}\|_{\ell^2}\leq\mathbf{0.2}\},$$

where $\partial\Omega_1=\{\|\mathbf{x_0}-\mathbf{x}\|_{\ell^2}=\mathbf{0.2}\}$, $\partial\Omega_0=\{x=0\}$, $\mathbf{x_0}=(\mathbf{0.5},\mathbf{0.5})$, and $\boldsymbol{\beta}=(v_0,0)$ with $v_0\geq 0$. This form of the Burgers equation retains the simplicity of its 1D counterpart and allows for more realistic 2D numerical tests.

We select an entropy solution to this problem by taking the limit as $t\to+\infty$ of the solution to the time-dependent version of (4.17), using as initial data the solution to the following problem:

$$\nabla^2 u_0=0,\quad u_0|_{\partial\Omega_1}=1,\quad u_0|_{\partial\Omega_0}=0,\quad \partial_n u_0|_{\partial\Omega_N}=0,$$

where $\partial\Omega_N$ is the complement of $\partial\Omega_0\cup\partial\Omega_1$.

The L^1 approximation is computed iteratively by solving the time-dependent problem, using the implicit Euler time-stepping. We test two configurations, $v_0=6$ and $v_0=4/3$, henceforth referred to as case 1 and case 2, respectively. To assess the accuracy of the method and its sensitivity to mesh refinement, we first do the computation on a uniform grid, $h=1/40$; then we redo it on a somewhat adapted grid with $1/10\leq h\leq 1/100$.

The results for case 1 are shown in Figure 11. We show the contour lines of the solution. Essentially, the exact solution consists of two regions where u is either equal to 1 or equal to 0, and these two regions are separated by a shock. Note that there is no shock in the upstream region and the $u=0$ solution reaches the cylinder. This means that the boundary condition $u|_{\partial\Omega_1}=1$ is satisfied in the entropy sense as defined in (4.12). We observe that the numerical solution satisfies the maximum principle and the contour lines are concentrated in the shock region. In this case the shock spreads over 2 to 3 elements; the reason for this is that the shock is almost aligned with the flow. This phenomenon is comparable to the smearing observed in the transport problem described in section 4.4. Smearing of oblique shocks is a common feature of techniques dealing with shocks. Note that the position of the shock does not change significantly as the mesh is refined, thus demonstrating that the coarse uniform mesh predicts quite well the position of the shock in question.

The contour lines of the numerical solution to case 2 are shown in Figure 12. Once more, the numerical solution is not plagued by spurious over- or undershootings. The

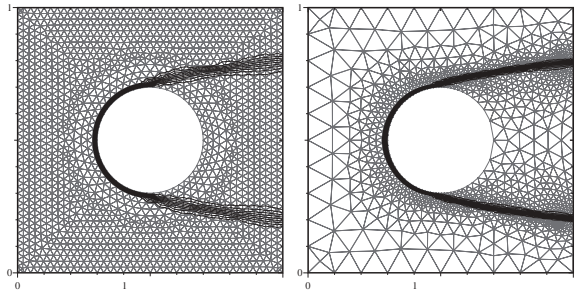

FIG. 11. *The Burgers equation with* $v_0 = 6$. *Contour lines of the solution. Left: uniform mesh* $h = 1/40$*; right: nonuniform mesh* $1/10 \leq h \leq 1/100$.

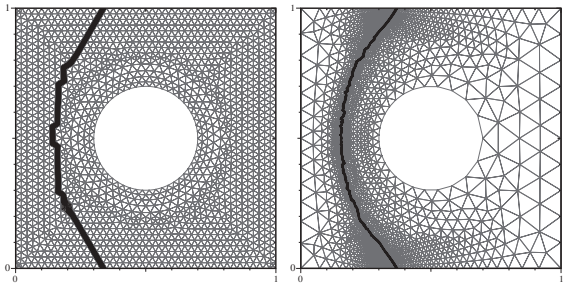

FIG. 12. *The Burgers equation with* $v_0 = 4/3$. *Contour lines of the solution. Left: uniform mesh* $h = 1/40$*; right: nonuniform mesh* $1/10 \leq h \leq 1/100$.

shock is almost perpendicular to the incoming flow; as a result, there is no smearing. The shock is a.e. contained within one element only.

The two above examples show that the L^1 technique is capable of selecting the entropy solution of Burgers-like equations. Moreover, the L^1 solution seems to satisfy a maximum principle. These two numerical observations are still to be understood and possibly proved mathematically.

5. Concluding remarks. One of the objectives driving the present work is to show that for solving first-order PDEs supplemented with nonsmooth data the ongoing debate pitting methods based on continuous interpolation against those based on discontinuous ones (e.g., H^1-conformal Galerkin vs. discontinuous Galerkin) is possibly pointless, insofar as the analysis is usually restricted to the $L^2(\Omega)$ setting. In the present paper, we have tried to promote the idea that working in a functional setting that provides for the right stability properties is as important as debating on the nature of the approximation (interpolation) space. Once the required stability property is guaranteed by the functional setting, the only requirement set for the discrete space is that it possesses good interpolation properties. As an illustration of this point of view, we have shown that, when working in $L^1(\Omega)$, the often despised continuous $\mathbb{P}_1$ finite element is capable of accurately approximating shocks, shear-layers, and boundary layers.

For reasons not yet completely clear, it seems that the $L^1(\Omega)$ approximation technique is capable of selecting viscosity solutions of first-order PDEs [5, 27] without resorting to any artificial artifact and/or tuning parameter, though this conjecture has yet to be substantiated mathematically.

All that has been said in this paper can be extended to spaces that are more exotic than the L^p's. For instance, we could consider Besov spaces or Radon measures, provided the corresponding norms can be computed efficiently in the discrete space E_h. While these spaces may provide better interpolation or approximation properties, they would require the use of wavelet bases or other hierarchical approximation spaces (for researches going in this direction, we refer the reader to, e.g., [7, 8]).

The generalization of the present work to evolution equations and conservation laws is under investigation and will be reported in a forthcoming paper.

Acknowledgments. The author acknowledges discussions with P. Azerad, J.T. Oden, B. Perthame, and L. Quartapelle that greatly improved the content of the present paper.

REFERENCES

[1] P. Azerad and G. Pousin, *Inégalité de Poincaré courbe pour le traitement variationnel de l'équation de transport*, C. R. Acad. Sci. Paris Sér. I Math, 322 (1996), pp. 721–727.

[2] A. K. Aziz, R. B. Kellogg, and A. B. Stephens, *Least-squares methods for elliptic systems*, Math. Comp., 44 (1985), pp. 53–70.

[3] C. Baiocchi, F. Brezzi, and L. P. Franca, *Virtual bubbles and Galerkin-Least-Squares type methods (GaLS)*, Comput. Methods Appl. Mech. Engrg., 105 (1993), pp. 125–141.

[4] C. Bardos, D. Brézis, and H. Brézis, *Perturbations singulières et prolongements maximaux d'opérateurs positifs*, Arch. Rational Mech. Anal., 53 (1973), pp. 69–100.

[5] C. Bardos, A. Y. Leroux, and J.-C. Nédélec, *First order quasilinear equations with boundary conditions*, Comm. Partial Differential Equations, 4 (1979), pp. 1017–1034.

[6] P. Benilan, H. Brezis, and M. G. Crandall, *A semilinear equation in $L^1(R^N)$*, Ann. Scuola Norm. Sup. Pisa Cl. Sci. (4), 2 (1975), pp. 523–555.

[7] J. H. Bramble, J. E. Pasciak, and P. S. Vassilevski, *Computational scales of Sobolev norms with application to preconditioning*, Math. Comp., 69 (2000), pp. 463–480.

[8] J. H. Bramble, R. D. Lazarov, and J. E. Pasciak, *A least-squares approach based on a discrete minus one inner product for first order systems*, Math. Comp., 66 (1997), pp. 935–955.

[9] J. H. Bramble and A. H. Schatz, *Rayleigh-Ritz-Galerkin-methods for Dirichlet's problem using subspaces without boundary conditions*, Comm. Pure Appl. Math., 23 (1970), pp. 653–675.

[10] J. H. Bramble and A. H. Schatz, *Least squares for 2mth order elliptic boundary-value problems*, Math. Comp., 25 (1971), pp. 1–32.

[11] H. Brezis and W. A. Strauss, *Semi-linear second-order elliptic equations in L^1*, J. Math. Soc. Japan, 25 (1973), pp. 565–590.

[12] H. Brezis, *Analyse fonctionnelle. Théorie et applications*, Applied Mathematics Series for the Master's Degree, Masson, Paris, 1983.

[13] F. Brezzi, M. O. Bristeau, L. P. Franca, M. Mallet, and G. Rogé, *A relationship between stabilized finite element methods and the Galerkin method with bubble functions*, Comput. Methods Appl. Mech. Engrg., 96 (1992), pp. 117–129.

[14] F. Brezzi, L. P. Franca, T. J. R. Hughes, and A. Russo, $b = \int g$, Comput. Methods Appl. Mech. Engrg., 145 (1997), pp. 329–364.

[15] F. Brezzi, P. Houston, D. Marini, and E. Süli, *Modeling subgrid viscosity for advection-diffusion problems*, Comput. Methods Appl. Mech. Engrg., 190 (2000), pp. 1601–1610.

[16] A. N. Brooks and T. J. R. Hughes, *Streamline upwind/Petrov–Galerkin formulations for convective dominated flows with particular emphasis on the incompressible Navier–Stokes equations*, Comput. Methods Appl. Mech. Engrg., 32 (1982), pp. 199–259.

[17] B. Cockburn, G. E. Karniadakis, and C. W. Shu, *Discontinuous Galerkin Methods - Theory, Computation and Applications*, Lect. Notes Comput. Sci. Eng. 11, Springer-Verlag, Berlin, 2000.

[18] A. Ern and J.-L. Guermond, *Elements finis: Théorie, applications, mise en œuvre*, Math. Appl. (Berlin) 36, Springer-Verlag, Paris, 2002.

[19] K. O. Friedrichs, *Symmetric positive linear differential equations*, Comm. Pure Appl. Math., 11 (1958), pp. 333–418.

[20] J.-L. Guermond, *Stabilisation par viscosité de sous-maille pour l'approximation de Galerkin*

des opérateurs linéaires monotones, C. R. Acad. Sci. Paris Sér. I Math., 328 (1999), pp. 617–622.

[21] J.-L. Guermond, *Stabilization of Galerkin approximations of transport equations by subgrid modeling*, M2AN Math. Model. Numer. Anal., 33 (1999), pp. 1293–1316.

[22] T. J. R. Hughes and M. Mallet, *A new finite element formulation for computational fluid dynamics.* IV: *A discontinuity-capturing operator for multidimensional advective-diffusive systems*, Comput. Methods Appl. Mech. Engrg., 58 (1986), pp. 329–336.

[23] B.-N. Jiang, *Non-oscillatory and non-diffusive solution of convection problems by the iteratively reweighted least-squares finite element method*, J. Comput. Phys., 105 (1993), pp. 108–121.

[24] B.-N. Jiang, *The Least-Squares Finite Element Method*, Scientific Computation, Springer-Verlag, Berlin, 1998.

[25] C. Johnson, U. Nävert, and J. Pitkäranta, *Finite element methods for linear hyperbolic equations*, Comput. Methods Appl. Mech. Engrg., 45 (1984), pp. 285–312.

[26] C. Johnson and A. Szepessy, *On the convergence of a finite element method for a nonlinear hyperbolic conservation law*, Math. Comp., 49 (1987), pp. 427–444.

[27] S. N. Kružkov, *First order quasilinear equations with several independent variables*, Mat. Sb. (N.S.), 81 (1970), pp. 228–255.

[28] J. E. Lavery, *Nonoscillatory solution of the steady-state inviscid Burgers' equation by mathematical programming*, J. Comput. Phys., 79 (1988), pp. 436–448.

[29] J. E. Lavery, *Solution of steady-state one-dimensional conservation laws by mathematical programming*, SIAM J. Numer. Anal., 26 (1989), pp. 1081–1089.

[30] J. E. Lavery, *Solution of steady-state, two-dimensional conservation laws by mathematical programming*, SIAM J. Numer. Anal., 28 (1991), pp. 141–155.

[31] P. Lesaint and P.-A. Raviart, *On a finite element method for solving the neutron transport equation*, in Mathematical Aspects of Finite Elements in Partial Differential Equations, C. de Boors, ed., Academic Press, New York, 1974, pp. 89–123.

[32] R. B. Lowrie and P. L. Roe, *On the numerical solution of conservation laws by minimizing residuals*, J. Comput. Phys., 113 (1994), pp. 304–308.

[33] A. I. Pehlivanov, G. F. Carey, and R. D. Lazarov, *Least-squares mixed finite elements for second-order elliptic problems*, SIAM J. Numer. Anal., 31 (1994), pp. 1368–1377.

[34] R. E. Showalter, *Monotone Operators in Banach Spaces and Nonlinear Partial Differential Equations*, Math. Surveys Monogr. 49, AMS, Providence, RI, 1996.

[35] E. Tadmor, *Convergence of spectral methods for nonlinear conservation laws*, SIAM J. Numer. Anal., 26 (1989), pp. 30–44.

[36] K. Yosida, *Functional Analysis*, Classics in Mathematics, Springer-Verlag, Berlin, 1995.